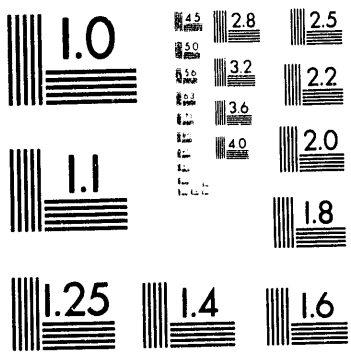
1.0
2.8
2.5
3.2
2.2
3.6
2.0
4.0
1.1
1.8
1.25
1.4
1.6

1 of 1

Conf-9311104--5

FABRICATION AND CHARACTERIZATION OF NANO-CRYSTALLINE DIAMOND FILMS*

Dieter M. Gruen, Xianzheng Pan, Alan R. Krauss,
Shengzhong Liu, Jianshu Luo, and Christopher M. Foster

Materials Science and Chemistry Divisions
Argonne National Laboratory
Argonne, IL 60439

To be presented at the

40th National Symposium and Topical Conferences
of the American Vacuum Society,
Orlando, FL

November 15-19, 1993

The submitted manuscript has been authored by a contractor of the U. S. Government under contract No. W-31-109-ENG-38. Accordingly, the U. S. Government retains a nonexclusive, royalty-free license to publish or reproduce the published form of this contribution, or allow others to do so, for U. S. Government purposes.

*Work supported by the U.S. Department of Energy, BES-Materials Sciences, Division of Advanced Energy Projects, under Contract W-31-109-ENG-38.

MASTER

FABRICATION AND CHARACTERIZATION OF NANO-CRYSTALLINE DIAMOND FILMS*

Dieter M. Gruen, Xianzheng Pan, Alan R. Krauss, Shengzhong Liu,

Jianshu Luo, and Christopher M. Foster

Materials Science/Chemistry Division, Argonne National Laboratory, 9700 S. Cass Avenue, Argonne, IL 60439-4831

ABSTRACT

Highly uniform, smooth nano-crystalline diamond films have been fabricated with a magneto-active microwave CVD system. The top and bottom magnet currents were 145A and 60A, respectively while the microwave power and the substrate temperature were controlled at 1500W and 850°C respectively during the deposition. The total processing pressure was regulated at 40 Pa (300 mTorr). with gas flow rates of 30 sccm of hydrogen, 2.4 sccm of methane and 1 sccm of oxygen. Diamond films obtained under the above conditions have grain sizes between 0.1-0.3 μm, a growth rate of 0.1μm/hr and a mean roughness of 14.95 nm. Characterization techniques have involved XRD, Raman spectroscopy, SEM, AFM and TEM. Both X-ray and electron diffraction patterns show no evidence of non-diamond phases.

---

* Work supported by the U. S. Department of Energy, BES-Material Science, Division of Advanced Energy Projects, under Contract W-31-109-ENG-38.

Although a high density of twins and stacking faults were revealed by HREM, compact diamond grains and clean intergranular boundaries (no graphitic or amorphous phases) were observed.

I. INTRODUCTION

Diamond possesses various unique properties, such as extreme hardness, high electrical resistance, chemical inertness and excellent thermal conductivity, among others. Upon doping, it becomes a large band gap semiconductor, manifesting extremely high breakdown voltage and high carrier mobility. In addition, it is transparent over a wide wavelength range, can withstand high electromagnetic radiation power fluxes from laser beams and X-ray sources, and be subjected to high pressures and high temperatures. Such outstanding properties make diamond of potential interest for a wide range of applications including heat spreaders, wear-resistant and transparent protective coatings for optical components, and novel semiconductor devices for microelectronics . Some of the techniques for diamond deposition in use today involve hot filament, oxy-acetylene torch or microwave plasma CVD processes. The resultant films are frequently nonuniform over large areas and the surfaces are very rough.

To overcome such problems, various approaches have been examined including the use of magneto-active microwave plasmas [1-4] at pressures ranging from 13.3 Pa (100 mTorr) to 2.66×10^3 Pa (20 Torr). In particular, at the lower pressures, the mean free path of electrons becomes longer, thus enabling one to increase the plasma density by magnetic confinement, thereby achieving uniform deposition over a large area.

In the present study, a magneto- active microwave plasma CVD system was used to produce smooth, uniform, nanocrystalline diamond films from CH_4-O_2-H_2 gas mixtures at a total pressure of 40 Pa. Detailed characterizations has involved SEM, AFM, XRD and Micro-Raman Spectroscopic techniques. In particular, TEM and HREM .have been used, apparently for the first time to investigate micro-structures of microwave CVD diamond films produced in the low pressure CVD regime.

II. EXPERIMENTAL

Diamond Deposition Condition

A commercial ASTeX PDS-17 microwave plasma deposition system was used for the diamond growth. Fig. 1 shows a schematic diagram of the ASTeX system , consisting of a six-way vacuum chamber, a graphite susceptor to which an induction heater and a thermocouple are attached, a 5000 W microwave power supply (2.45 GHz), two magnets, gas handling and vacuum pumping systems and their computerized control devices. The computer also includes data logging capability with on-line data trending. The window and exit magnet currents were set at 145 A and 60 A respectively, while the microwave power and the substrate temperature were controlled at 1500 W and 850°C respectively during the deposition. After the reaction chamber was evacuated to a base pressure of 1.33×10^{-4} Pa (10^{-6} Torr), a gas flow of 30 sccm of hydrogen, 2.4 sccm of methane and 1 sccm of oxygen was introduced to the chamber. The total processing pressure was regulated at 40 Pa (300 mTorr).

Si substrates were supplied either by ASTeX or were prepared at ANL by vibration polishing under a load of 45g/cm^2, using 0.1μm diamond powder. After polishing, the Si wafers were rinsed with acetone and methyl alcohol.

Characterization

The microstructure of the films was investigated using a JEOL JXA-840A scanning electron microscope (SEM) and a Nanoscope III atomic force microscope (AFM). The crystal structure was investigated using X-ray diffraction (XRD) on a Phillips powder diffractometer. Raman spectra were obtained using a Coherent Innova 90 Ar^+ ion laser and a Spex 1401 double grating monochromator. The system used cooled (-60°C) RCA C31034A photomultiplier tubes as the detectors in a single-channel, photon counting mode. Samples were mounted in a Hi-Tran gas flow cryostat with the laser light focused and collected by an achromatic lens. The spectral resolution was ~0.5 cm^{-1}.

Plan-view TEM specimens were prepared by cutting the silicon-supported film into 1.5 x 1.5 mm sections with a diamond saw. The silicon substrate was removed chemically by immersing the specimen in a solution of 11% HF, 11% HNO_3, and 78% CH_3COOH. The free diamond film was then carefully affixed to a copper grid having a hole at the center, followed by ion-milling until the film was perforated using 6 kV Ar^+ with a beam incidence angle of ~13°. Transmission electron microscopy (TEM) and electron diffraction were performed on a Philips CM 30 microscope, operating at 300 kV. For high-resolution electron microscopy (HREM), a JEOL 4000EX was utilized, which has a point to point resolution of 1.65 Å at 400 kV with a biaxial tilt of ~20°. The crystals were tilted to an exact <110> orientation for image recording.

III. RESULTS AND DISCUSSION

Diamond films obtained under the above conditions are essentially polycrystalline with high resistivity (>1.2 x 10^{10} Ω-cm) and small grain size, (0.1-0.3 μm). Both the X-ray and electron diffraction patterns show no evidence of a graphitic phase. Although a high density of twins, dislocations and stacking faults was revealed by TEM and HREM, compact diamond grains and clean intergranular boundaries were observed throughout. Raman spectroscopy revealed a peak at 1332 cm^{-1} which evidences the presence of the diamond phase.

As shown in figure 2, the diamond [111], [220] and [311] diffraction peaks were clearly observed in XRD. In addition, no graphite diffraction peaks were detected. The diffraction data therefore demonstrate that high quality diamond films were produced. However, careful examination reveals that the ratio of the [220] peak intensity to that of the [111] peak is 1:2.5 while the expected ratio for polycrystalline diamond is 4:1. The 1:2.5 ratio suggests a predominant [220] orientation. Although the 1:2.5 intensity ratio observed in our samples is reproducible, rocking curve measurements show no angular dependence, indicating a lack of texturing. Electron diffraction and high resolution TEM imaging also do not give evidence for texturing. We believe that X-ray diffraction results are not sufficient in our case to warrant the conclusion that texturing occurs in these nano-crystalline films. Other ancillary experiments are therefore necessary before such a conclusion can be reached.

A Raman spectrum for our deposits is shown in figure 3. A peak centered at 1332 cm^{-1}, characteristic of diamond, is observed. The full width at half maximum (FWHM) of this peak is 25 cm^{-1}, about eight times wider than that

of natural diamond (3.3 cm^{-1}) [5]. A broad peak with a maximum at 1500 cm^{-1}, which is usually attributed to nondiamond carbon phases, is also observed. The ratio of intensity of the 1500 cm^{-1} peak to that of the 1332 cm^{-1} peak I_c / I_d is about 1.15. It has been reported that the Raman sensitivity for amorphous carbon is roughly 50 times that of diamond [5, 6, 7]. Thus the peak at 1500 cm^{-1} is perhaps indicative of small amounts (< 2.5%) of amorphous carbon in the deposits. The diamond component certainly dominated the film composition, and the XRD, TEM and electron diffraction data support this conclusion.

The film morphology as observed by SEM is shown in Fig. 4 (a) --plan-view surface and Fig. 4(b)--cross section. Fig. 4(a) reveals that the film is smooth, continuous and consists of coalesced crystallites that are extremely fine grained. The cross sectional view indicates both a columnar morphology and increasing grain size as the film thickness increases. The thickness is about 1.7 μm, and the growth rate is nearly 0.1 μm/ hr. Fig.4(c) presents the AFM image (bottom) and a surface topographical analysis (top) of the film. The film is very smooth with an RMS roughness of 14.95 nm.

TEM observations (Fig. 5), show a relatively uniform grain size distribution. The intergranular boundaries appeared very clean, and there was no evidence of segregation or the presence of secondary phases. The difference in contrast between individual grains is attributed to differences in their orientation with respect to the incident electron beam. Selected area diffraction (SAD) taken from different areas of the film revealed a polycrystalline pattern (Fig 6), which could be completely indexed to an FCC diamond structure. The measured d spacings were within 5% of the published values and within experimental error for this type of measurement.

TEM showed that each submicron diamond grain contained a high density of structural defects (Fig. 7). The predominant defects appeared to be {111} twins as identified by SAD from single diamond grains. Another type of planar defect that is frequently observed in our work are stacking faults (see Fig. 7). Figure 8 shows an SAD diffraction pattern from a single grain. Two sets of diffraction spots from the matrix and twin were clearly observed. Streaking of the SAD pattern was also observed and was attributed to the presence of micro twins consisting of just a few atomic planes, which lie in a direction normal to the {111} twin plane. These types of defects have been previously observed in diamond films that had been prepared by using different techniques. Walmsley et al. [8] reported twins existed in high pressure/high temperature grown diamonds. W. Zhu et al. [9] investigated by TEM the structural imperfections in high pressure CVD diamond films and found that the diamond films contained a large number of stacking faults and twins that lie on the {111} planes. The strong tendency of forming these structural imperfections was attributed to the small activation energy involved in defect formation [9].

Figure 9 is a high resolution image of a twinned diamond crystal along the [110] axis. The micro twins observed were only several atom planes thick and tended to form bands that lay perpendicular to the twin plane. It is interesting to note that some of these bands end in the middle of the crystal (see Fig. 9). The majority of the twin boundaries were of $\Sigma 3$ type using the coincidence site lattice notation [10]. The intersections of these twin boundaries were also frequently observed in the crystal, leading to the formation of higher order boundaries. Figure 10 provides a closer look of such an intersection. In this case, as many as four twins meet together and form a complicated boundary configuration. Shechtman et al.[11] studied the interaction of twins in diamond

crystals and found that the meeting points of $\Sigma 3$ twins were very important for the nucleation and growth of diamond crystals. A demonstration of the effect of twinning on the growth in the diamond crystal has also been given in the literature [12]. It is claimed that the vertices or edges of such twinned regions provide the nucleation sites for the new planes [10, 12].

V. SUMMARY

Diamond films have been prepared using CH_4-H_2-O_2 gas mixtures at a total process pressure of 40 Pa (300 mTorr) in a magneto-active microwave system. Raman and XRD measurements demonstrated that the film is good quality diamond. SEM and AFM revealed small (0.1-0.3 μm) grain size and roughness (RMS=14.95 nm), leading to the conclusion that uniform and smooth diamond films were produced. The growth rate is about 0.1 μm / hr. TEM images displayed a high density of defects such as dislocations, stacking faults and twins. HREM revealed that intergranular boundaries were clean with no evidence for the presence of non-diamond phases, consistent with the XRD and Micro Raman characterizations.

V. ACKNOWLEDGMENTS.

The authors would like to thank Dr. Orlando Auciello of the MCNC Microelectronics Center of N. Carolina for doing the AFM measurement.

References:

1. M.Komori, T. Maki, T. Kim, G. L. Hou, Y. Sakaguchi, K. Sakuta and T..Kobayashi, Appl. Phys. Lett. **62** ,582 (1993).

2. Shu Jin and T.D. Moustakas, Diamond and Related Materials, **2**, 1355(1993).

3. M. Yuasa, O. Arakaki, J.S.Ma, A.Hiraki, and H.Kawarada, Diamond and Related Materials.**1**,168(1992).

4. J.Suzuki, H.Kawarada, K.Max, J.wei, Y.Yokota and A.Hiraki, Jap. J. Appl. Phys. **28,** L 281(1989).

5 C.R.Eddy, Jr., D.L.youchison, B.D.Sartwell and K.S.Grabowski J. Mater. Res., **7**,3255(1992).

6. R.J.Nemanich, J.T.Glass, G.Lucovsky, and R.E.Shroder , J. Vac. Sci. Tech. **A6**,1783 (1988).

7. N.Wada, S.A. Solin, Physica , **105B**,353(1981).

8. J. C. Walmsley and A. R. Lang, J. Mater. Sci. Lett. **2**, 785 (1983).

9. W. Zhu, A. R Badzian, and R. Messier, J. Mater. Res. **4**, 659 (1989).

10. S. Ranganathan, Acta Crystallogr. **21**, 197 (1966).

11. D. Shecthman, J. L. Hutchison, L. H. Robins, E. N. Farabaugh, and A. Feldman, J. Mater. Res. **8**, 473 (1993).

12. D. R. Hamilton and R. G. Seidensticker, J. Appl. Phys. **34**, 1450 (1960).

Figure Caption

Fig. 1. Schematic diagram of magneto-microwave PACVD system.

Fig. 2. XRD scan of diamond film grown by magneto-microwave PACVD.

Fig. 3. Raman spectrum of diamond film deposited from magneto-microwave PACVD.

Fig. 4(a). Surface SEM micrography of diamond film

Fig. 4(b). Cross section SEM micrography of diamond film.

Fig. 4(c) AFM image (bottom) and surface topographicals analysis (top) of diamond film.

Fig. 5. Plan-view TEM image of the polycrystalline diamond film prepared using magneto-microwave PACVD deposition.

Fig. 6. Typical selected area diffraction (SAD) pattern taken from the diamond film prepared using magneto-microwave PACVD deposition.

Fig. 7. TEM image reveals a high density of structural defects in a submicron diamond grain.

Fig. 8. Selected area diffraction (SAD) pattern taken along the [110] axis of a diamond crystal shows the presence of twins.

Fig. 9. High resolution electron microscopy (HREM) image of a twinned diamond crystal.

Fig. 10. High resolution electron microscopy (HREM) image of the interaction between several micro-twins in a heavily defected region.

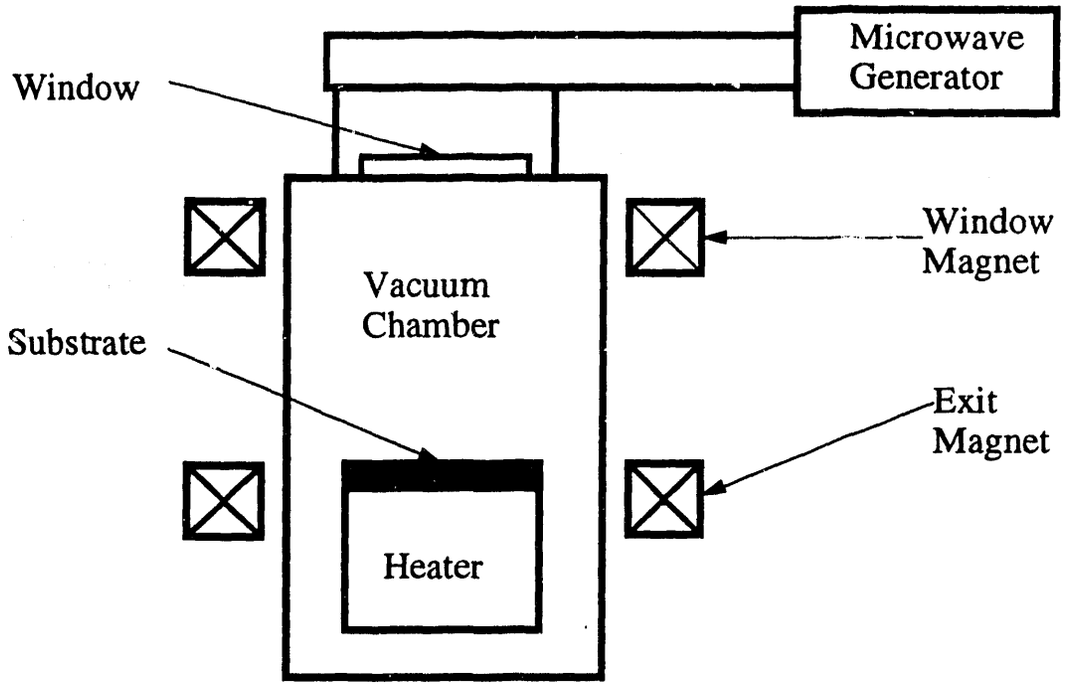

Fig. 1 Schematic diagram of magneto-microwave PACVD system.

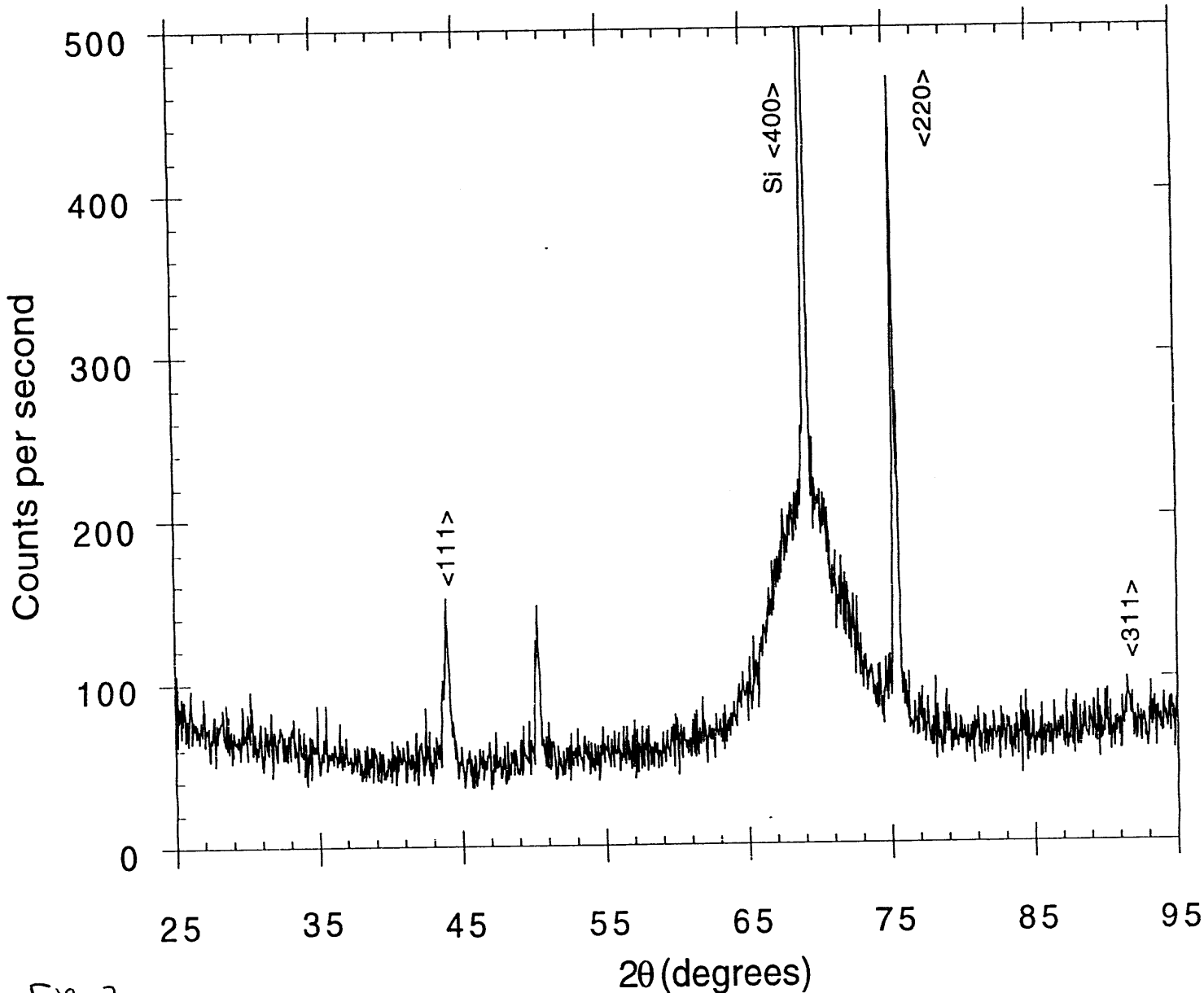
500
400
300
200
100
0
Counts per second
<111>
Si <400>
<220>
<311>
25
35
45
55
65
75
85
95
2θ (degrees)

Fig. 2

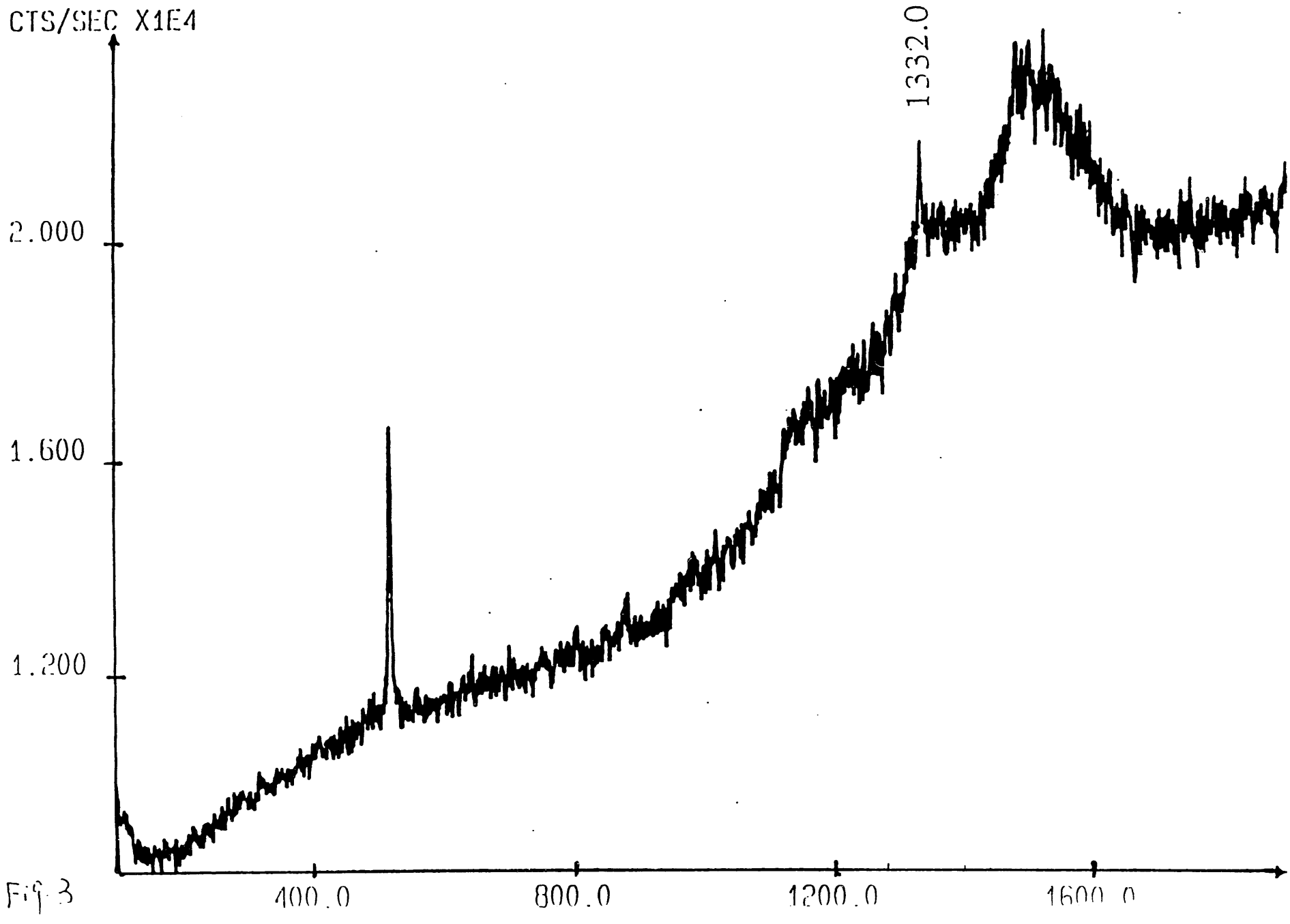

Fig 3

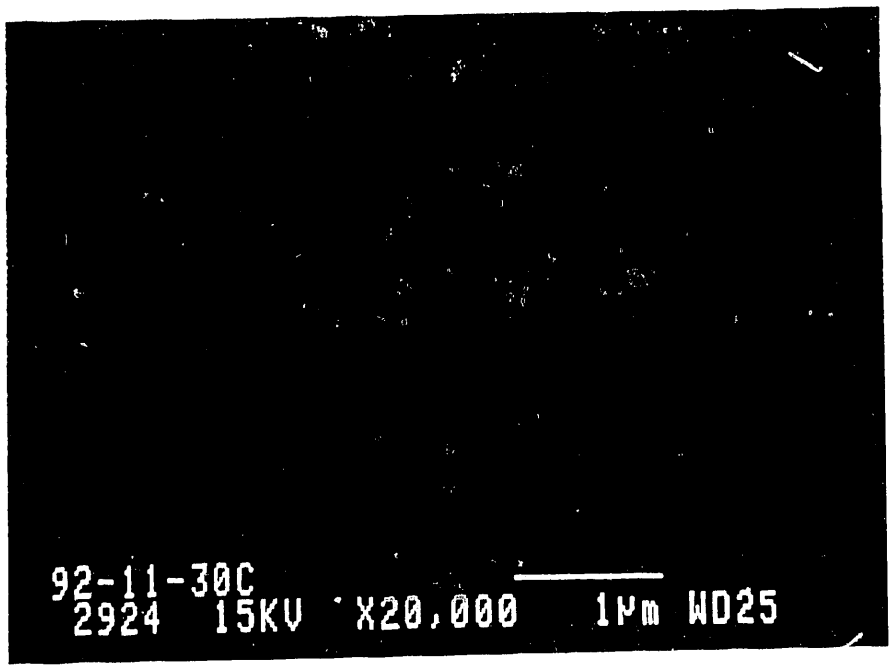

Fig.4(a)

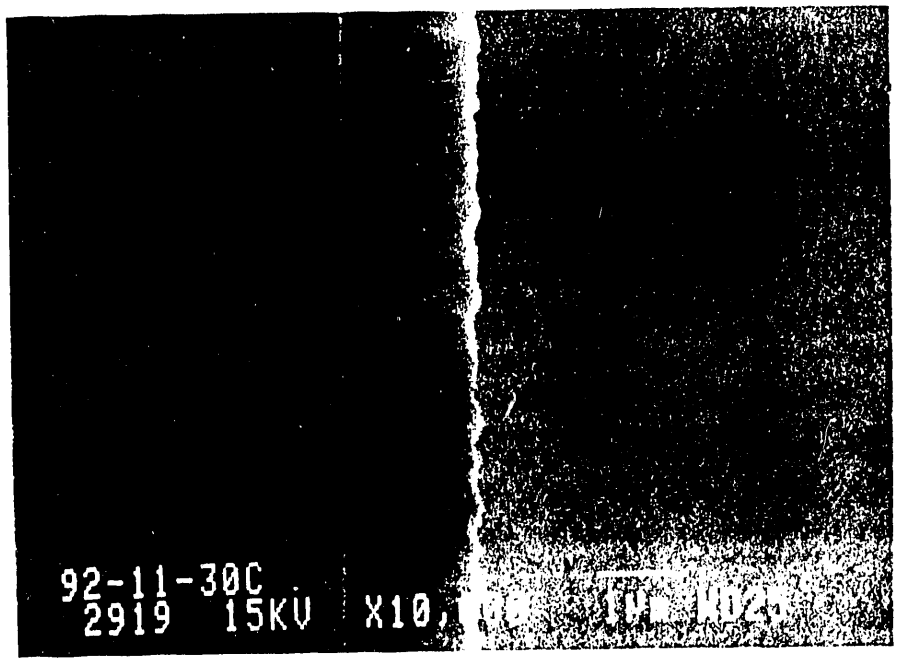

Fig.4(b)

Line Marker Spectrum Zoom Center Line Clear

Section Analysis

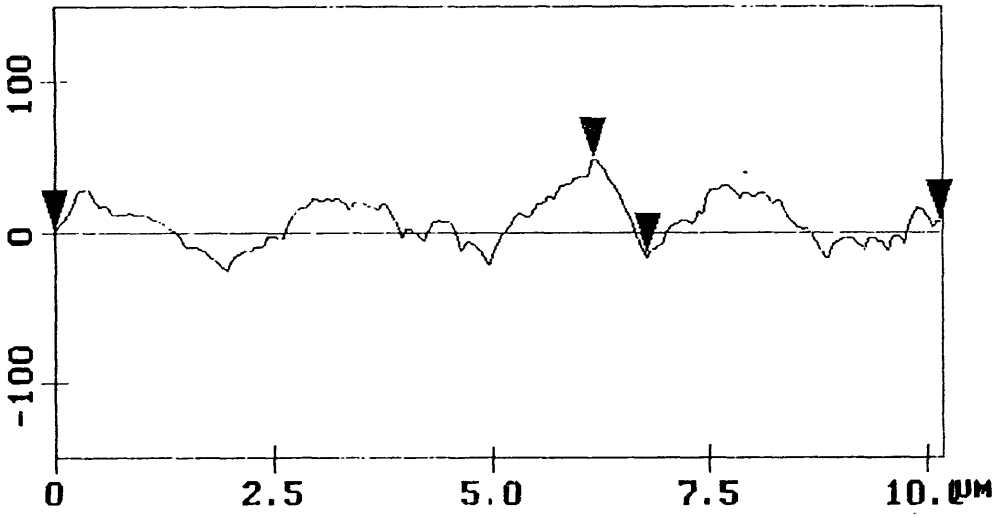

L	10.156 µm
RMS	14.952 nm
lc	DC
Ra(lc)	12.487 nm
Rmax	71.265 nm
Rz	43.741 nm
Rz Cnt	valid

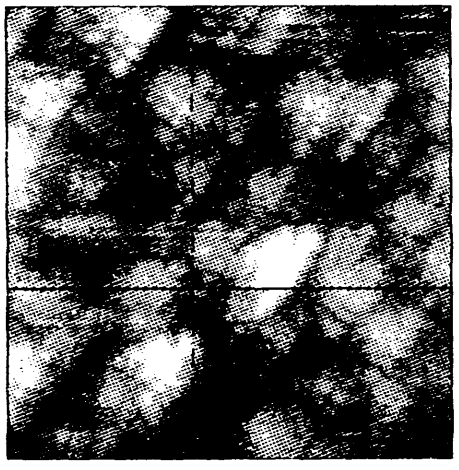

Moving line Zoom 2:1 Center line Off

Fig. 4(c)

Fig. 5

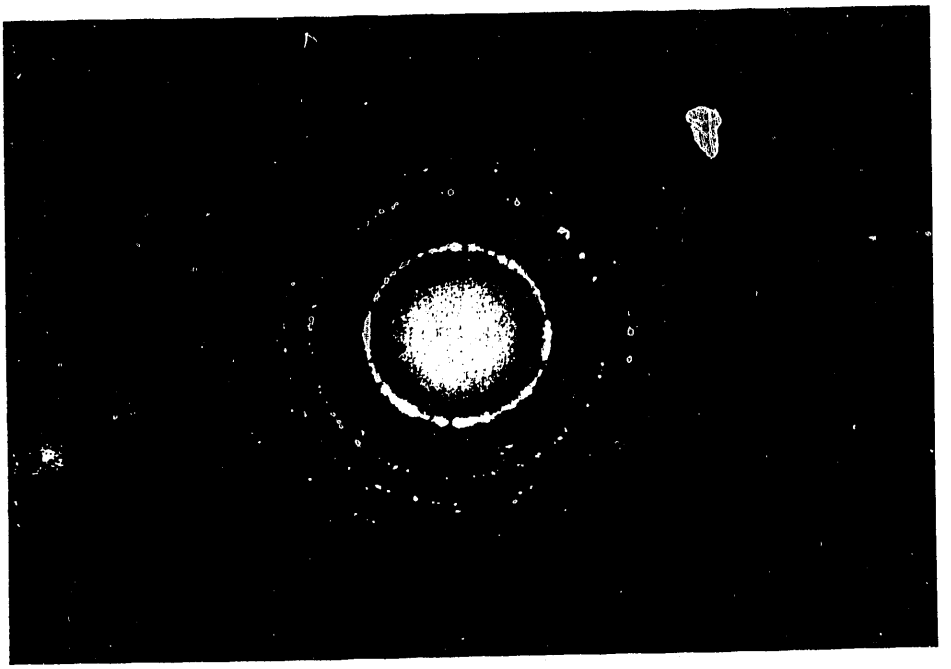

Fig. 6

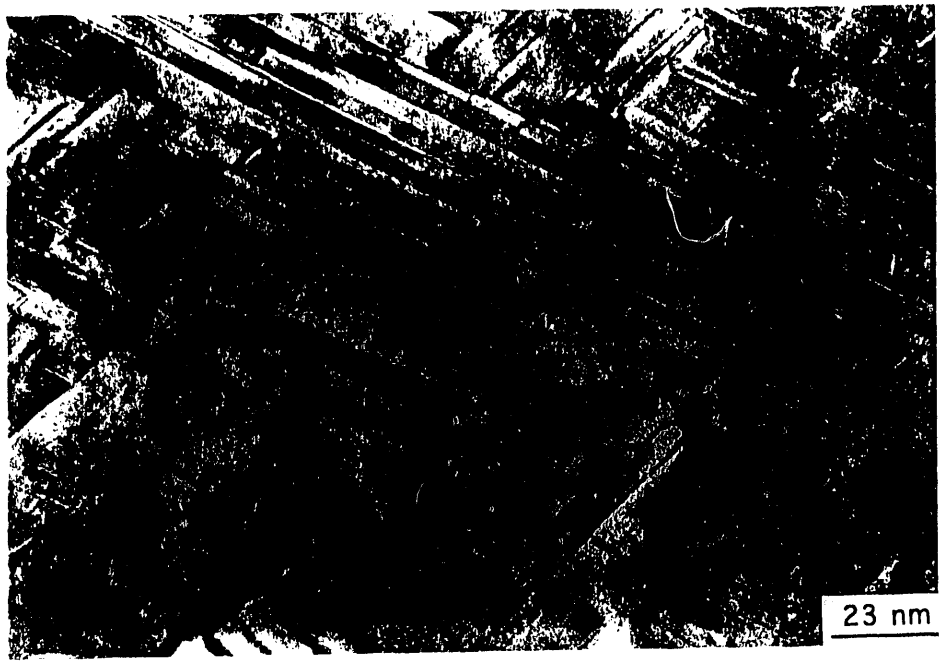

Fig. 7

Fig 8

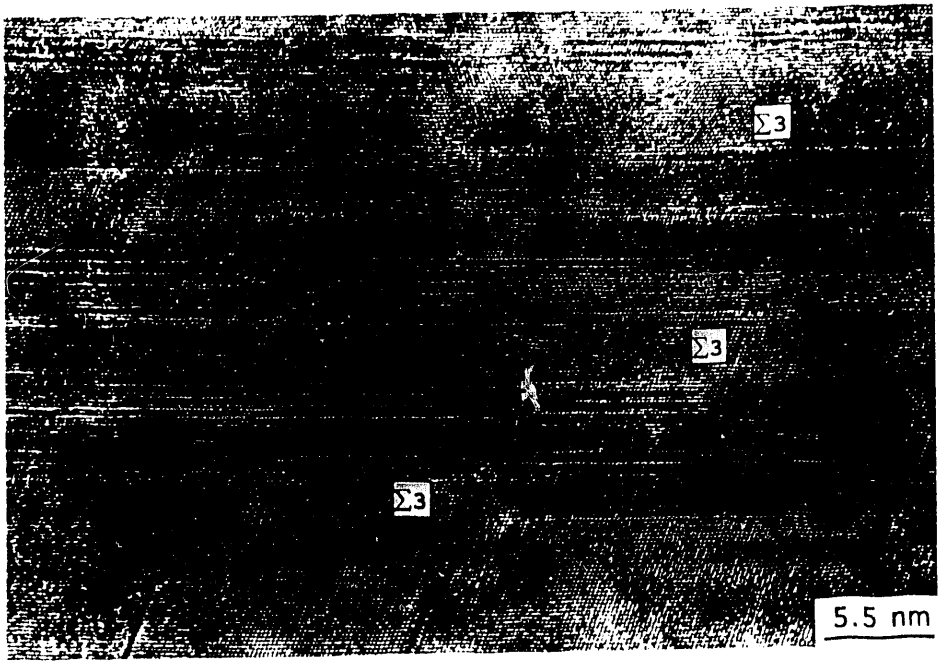

Fig. 9

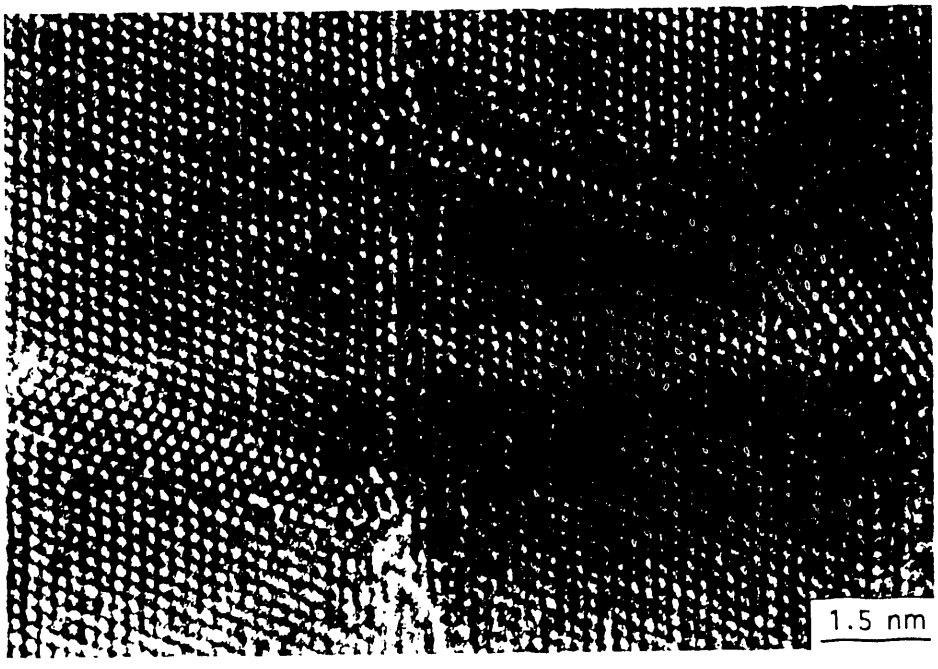

Fig. 10

DATE
FILMED
1/3/94

END